ISSN 0021-8944, Journal of Applied Mechanics and Technical Physics, 2016, Vol. 57, No. 3, pp. 463–472. © Pleiades Publishing, Ltd., 2016.
Original Russian Text © M. Kalteh, S. Ghorbani, T. Khademinejad.

VISCOUS DISSIPATION AND THERMAL RADIATION EFFECTS ON THE MAGNETOHYDRODYNAMIC (MHD) FLOW AND HEAT TRANSFER OVER A STRETCHING SLENDER CYLINDER

M. Kalteh[a], S. Ghorbani[a], and T. Khademinejad[b]

UDC 532.62

Abstract: An axisymmetric magnetohydrodynamic (MHD) boundary layer flow and heat transfer of a fluid over a slender cylinder are investigated numerically. The effects of viscous dissipation, thermal radiation, and surface transverse curvature are taken into account in the simulations. For this purpose, the governing partial differential equations are transformed to ordinary differential equations by using appropriate similarity transformations. The resultant ordinary differential equations along with appropriate boundary conditions are solved by the fourth-order Runge–Kutta method combined with the shooting technique. The effects of various parameters on the velocity and temperature profiles, local skin friction coefficient, and Nusselt number are analyzed.

Keywords: axisymmetric flow, stretching cylinder, viscous dissipation, thermal radiation, Runge–Kutta method.

DOI: 10.1134/S002189441603010X

INTRODUCTION

The problem of the flow and heat transfer of a fluid over a stretching surface is very important in engineering and industrial processes, such as hot rolling, polymer extrusion, wire coating, food processing, etc.

Crane [1] was the first one who focused on the flow of a fluid over a stretching plate. Gupta and Gupta [2] studied the influence of suction/injection on heat and mass transfer of the fluid. Grubka and Bobba [3] and Ali [4] analyzed the problem of the flow and heat transfer over a continuously stretching sheet with considering the linear stretching rate and wall temperature. Wang [5] analyzed the hydrodynamics of the flow over an unsteady stretching surface. Andersson and Dandapat [6] extended Crane's work to non-Newtonian power-law fluids. On the other hand, Andersson et al. [7] studied the momentum transfer in a thin liquid film of a power-law fluid on an unsteady stretching sheet, and the corresponding heat transfer problem was explored by Chen [8].

As mentioned above, the quality of the final product highly depends on the heating or cooling rate of the fluid during the process. Thus, Chamkha [9] presented an analysis of a hydromagnetic flow and heat transfer past a stretching sheet, and Abel et al. [10] considered viscous dissipation effects on heat transfer of a fluid under the influence of an external magnetic field. The problem of an unsteady mixed convection flow and heat transfer past a porous stretching sheet with considering thermal radiation effects was investigated by Mukhopadhyay [11]. In addition, Mukhopadhyay [12] examined the effects of variable viscosity and thermal diffusivity on a boundary layer flow and heat transfer over a porous stretching sheet. The effect of a nonuniform heat source on fluid heat transfer over a porous stretching sheet was determined by Tsai et al. [13]. Some other researchers carried out similar studies for non-Newtonian power-law fluids [14–18].

[a]Department of Mechanical Engineering, University of Guilan, 3756 Rasht, Iran; mkalteh@guilan.ac.ir; ghorbanisaba@gmail.com. [b]Department of Mechanical and Aerospace Engineering, Illinois Institute of Technology, 60616 Chicago, USA; tkhademi@hawk.iit.edu. Translated from Prikladnaya Mekhanika i Tekhnicheskaya Fizika, Vol. 57, No. 3, pp. 84–95, May–June, 2016. Original article submitted February 26, 2014; revision submitted May 18, 2014.

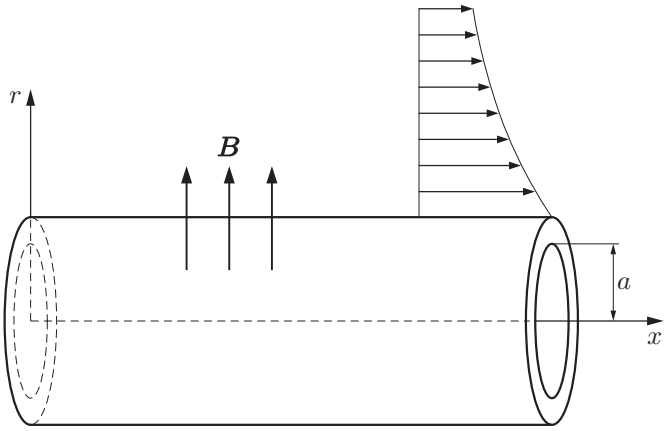

Fig. 1. Schematic representation of the problem.

Some studies were also performed for cylindrical geometry. Crane [19] investigated a boundary layer flow due to a stretching cylinder. Wang [20] extended Crane's work and considered a viscous fluid flow due to a stretching hollow cylinder in a quiescent fluid. Ishak et al. [21, 22] examined the effects of suction/injection and magnetic field on a steady flow and heat transfer of a fluid along a stretching cylinder without considering the transverse curvature. Zaimi et al. [23] analyzed an unsteady flow and mass transfer over a shrinking cylinder.

The transverse curvature parameter is defined as the ratio of the boundary layer thickness to the cylinder radius. For very small transverse curvature parameters, the problem can be solved in a two-dimensional formulation. For a slender cylinder, however, the problem becomes axisymmetric, and the surface transverse curvature parameter appears in the governing equations. Ishak and Nazar [24] proposed a similarity variable for the problem of the flow and heat transfer along a stretching slender cylinder. Later on, Bachok and Ishak [25] presented a numerical study of the flow and heat transfer over a horizontal cylinder with considering the effect of the transverse curvature parameter and prescribed surface heat flux. Vajravelu et al. [26] explored the influence of the temperature-dependent thermal conductivity on the flow and thermal boundary layer along a stretching slender cylinder. They also considered the external heat source and transverse magnetic field for two different thermal boundary conditions. Some other researchers carried out investigations on mixed convection over a vertical stretching slender cylinder [27, 28].

According to this background, it is clear that there is no sufficient information on the effect of thermal radiation and viscous dissipation on the flow and heat transfer along a stretching slender cylinder in the available literature. Hence, an MHD boundary layer flow and heat transfer of an incompressible fluid over a steady linearly stretching slender cylinder with a prescribed surface temperature is studied in the present work. The effects of thermal radiation, viscous dissipation, and Prandtl number on the temperature profile are also investigated.

MATHEMATICAL FORMULATION

Let us consider a Newtonian electrically conducting fluid around a slender cylinder with a prescribed surface temperature (Fig. 1). Surface stretching induces an incompressible laminar boundary layer flow in the x direction. The flow is also affected by an external radial magnetic field. The surface stretching rate U_w and the surface temperature T_w are defined as

$$U_w = bx/l, \qquad T_w = T_\infty + c(x/l)^s,$$

where b is the stretching velocity, l is the reference length, T_∞ is the quiescent fluid temperature, s is the prescribed surface temperature exponent, and c is a positive constant; the x axis coincides with the axial direction of the cylinder.

For an axisymmetric flow, the governing differential equations are the mass, momentum, and energy conservation equations

$$\frac{\partial (ru)}{\partial x} + \frac{\partial (rv)}{\partial r} = 0;$$

$$u\,\frac{\partial u}{\partial x}+v\,\frac{\partial u}{\partial r}=\nu\Big(\frac{\partial^2 u}{\partial r^2}+\frac{1}{r}\,\frac{\partial u}{\partial r}\Big)+\frac{1}{\rho}\,(\boldsymbol{j}\times\boldsymbol{B})_x; \tag{1}$$

$$\rho c_p\Big(u\,\frac{\partial T}{\partial x}+v\,\frac{\partial T}{\partial r}\Big)=\frac{1}{r}\,\frac{\partial}{\partial r}\Big(kr\,\frac{\partial T}{\partial r}\Big)+\Phi-\frac{1}{r}\,\frac{\partial\,(rq_r)}{\partial r}; \tag{2}$$

the boundary conditions can be written as

$$u=U_w,\quad v=0,\quad r=a,\qquad u=0,\quad r\to\infty,$$

$$T=T_w,\quad r=a,\qquad T=T_\infty,\quad r\to\infty,$$

where u and v are the velocity components in the x and r directions, respectively, T is the fluid temperature, and ν is the kinematic viscosity. The term $(\boldsymbol{j}\times\boldsymbol{B})_x$ in Eq. (1) is the x component of the Lorentz force produced by the external radial magnetic field in the form $\boldsymbol{B}=(B_0/r)\boldsymbol{e}_r$ $(\nabla\cdot\boldsymbol{B}=0)$.

As the magnetic Reynolds number is assumed to be small, the induced magnetic field is negligible [29]; consequently, according to Ohm's law, the electric current in the direction $\boldsymbol{e}_\theta$ is

$$j=\sigma[\boldsymbol{E}+\boldsymbol{V}\times\boldsymbol{B}]\boldsymbol{e}_\theta, \tag{3}$$

where $\boldsymbol{E}$ is the electric field intensity satisfying Maxwell's equations for a steady magnetic field with no charge:

$$\nabla\cdot\boldsymbol{E}=0\quad\Rightarrow\quad\boldsymbol{E}=E(r,x)\boldsymbol{e}_\theta$$

or

$$\boldsymbol{E}=E(r)\boldsymbol{e}_\theta=(c'/r)\boldsymbol{e}_\theta. \tag{4}$$

Here c' is a constant obtained by substituting Eq. (4) into Eq. (3) and then using Eq. (1) for the inviscid free stream:

$$u\,\frac{\partial u_\infty}{\partial x}+v\,\frac{\partial u_\infty}{\partial r}=\nu\Big(\frac{\partial^2 u_\infty}{\partial r^2}+\frac{1}{r}\,\frac{\partial u_\infty}{\partial r}\Big)-\frac{\sigma(c'B_0+u_\infty B_0^2)}{\rho r^2}\quad\Rightarrow\quad c'=0.$$

Thus, we obtain $\boldsymbol{j}\times\boldsymbol{B}=-(\sigma uB_0^2/r^2)\boldsymbol{e}_x$ for the Lorentz force, and Eq. (1) is simplified to

$$u\,\frac{\partial u}{\partial x}+v\,\frac{\partial u}{\partial r}=\nu\Big(\frac{\partial^2 u}{\partial r^2}+\frac{1}{r}\,\frac{\partial u}{\partial r}\Big)-\frac{\sigma uB_0^2}{\rho r^2}. \tag{5}$$

The term Φ in Eq. (2) represents the viscous dissipation contribution, which can be found as

$$\Phi=\mu\Big[2\Big(\Big(\frac{\partial v}{\partial r}\Big)^2+\Big(\frac{v}{r}\Big)^2+\Big(\frac{\partial u}{\partial x}\Big)^2\Big)+\Big(\frac{\partial v}{\partial x}+\frac{\partial u}{\partial r}\Big)^2\Big]. \tag{6}$$

In the boundary layer approximation, Eq. (6) reduces to

$$\Phi=\mu\Big(\frac{\partial u}{\partial r}\Big)^2. \tag{7}$$

Furthermore, according to the Rosseland approximation [30], thermal radiation is considered as a radiative heat flux in the r direction:

$$q_r=-\frac{4\sigma^*}{3k^*}\,\frac{\partial T^4}{\partial r} \tag{8}$$

(σ^* and k^* are the emissivity and the Boltzmann constant, respectively). The variable T^4 is expanded about T_∞ into the Taylor series

$$T^4\simeq T_\infty^4+4T_\infty^3(T-T_\infty)+6T_\infty^2(T-T_\infty)^2+\ldots,$$

which is reduced to the following equation by neglecting higher-order terms of $T-T_\infty$:

$$T^4\simeq 4T_\infty^3T-3T_\infty^4. \tag{9}$$

Substitution of Eq. (9) into Eq. (8) yields

$$q_r = -\frac{16T_\infty^3\sigma^*}{3k^*}\,\frac{\partial T}{\partial r}. \tag{10}$$

Substituting Eqs. (7) and (10) into Eq. (2), we obtain the energy balance equation

$$\rho c_p\Big(u\,\frac{\partial T}{\partial x} + v\,\frac{\partial T}{\partial r}\Big) = k\,\frac{1}{r}\,\frac{\partial}{\partial r}\Big(r\,\frac{\partial T}{\partial r}\Big) + \mu\Big(\frac{\partial u}{\partial r}\Big)^2 + \frac{16T_\infty^3\sigma^*}{3k^*}\,\frac{1}{r}\,\frac{\partial}{\partial r}\Big(r\,\frac{\partial T}{\partial r}\Big). \tag{11}$$

A dimensionless similarity variable of the form described in [24],

$$\eta = \frac{r^2 - a^2}{2a}\Big(\frac{U_w}{\nu x}\Big)^{1/2}, \tag{12}$$

is applied to transform the governing partial differential equations to first-order ordinary differential equations. The stream function is defined as

$$\psi = (\nu x U_w)^{1/2} a f(\eta). \tag{13}$$

The velocity components have the form

$$u = U_w f'(\eta), \qquad v = -\frac{a}{r}\Big(\frac{\nu b}{l}\Big)^{1/2} f(\eta). \tag{14}$$

At a prescribed surface temperature, the temperature profile θ is defined as

$$\theta = \frac{T - T_\infty}{T_w - T_\infty}. \tag{15}$$

Substituting Eqs. (12)–(15) into Eqs. (5) and (11), which can be solved numerically by the fourth-order Runge–Kutta method, we obtain the equations

$$ff'' - (f')^2 - \frac{M}{1+2\gamma\eta}\,f' + 2\gamma f'' + (1+2\gamma\eta)f''' = 0; \tag{16}$$

$$sf'\theta - f\theta' - \frac{1}{\mathrm{Pr}'}\left[2\gamma\theta' + (2\gamma\eta+1)\theta''\right] - \mathrm{Ec}\left[(2\gamma\eta+1)(f'')^2\right] = 0 \tag{17}$$

with the corresponding boundary conditions for the transformed velocity and temperature:

$$f'(0) = 1, \qquad f(0) = 0, \qquad f'(\infty) = 0,$$
$$\theta(0) = 1, \qquad \theta(\infty) = 0.$$

Here $\gamma = \sqrt{l\nu/(ba^2)}$ is the transverse curvature parameter, $M = \sigma B_0^2 l/(\rho a^2 b)$ is the magnetic field parameter, $\mathrm{Ec} = (U_w)^2/(c_p(T_w - T_\infty))$ is the Eckert number, $\mathrm{Pr}' = (1+N)/\mathrm{Pr}$ is the modified Prandtl number, $\mathrm{Pr} = \rho c_p\nu/k$ is the Prandtl number, and $N = 16T_\infty^3\sigma^*/(3kk^*)$ is the thermal radiation parameter; the local skin friction coefficient and local Nusselt number are defined by the expressions

$$C_{fx} = -2\tau_w/(\rho U_w^2) = -2f''(0)(\mathrm{Re}_x)^{-1/2}, \qquad \mathrm{Nu}_x = \frac{\partial\theta}{\partial\,(r/a)}\Big|_{r=a} = \frac{a}{x}\,(\mathrm{Re}_x)^{1/2}\theta'(0),$$

where $\mathrm{Re}_x = U_w x/\nu$ is the local Reynolds number.

It is important to note that Eqs. (16) and (17) can be simplified in special basic cases by omitting some of the parameters. For example, in the case with $\gamma = 0$, the problem can be reduced to the problem of the flow and heat transfer over a horizontal stretching sheet; under the assumption that $M = N = 0$, it is reduced to Crane's problem [1].

NUMERICAL PROCEDURE AND VALIDATION

To use the fourth-order Runge–Kutta method, Eqs. (16) and (17) should be reduced to a system of nonlinear first-order differential equations

$$\frac{df_0}{d\eta} = f_1, \quad \frac{df_1}{d\eta} = f_2, \quad \frac{df_2}{d\eta} = \frac{(M/(1+2\gamma\eta))f_1 + (f_1)^2 - f_0 f_2 - 2\gamma f_2}{1+2\gamma\eta},$$
$$\frac{d\theta_0}{d\eta} = \theta_1, \qquad \frac{d\theta_1}{d\eta} = \frac{\mathrm{Pr}'\left[sf_1\theta_0 - f_0\theta_1 - \mathrm{Ec}\,(1+2\gamma\eta)(f_2)^2\right] - 2\gamma\theta_1}{1+2\gamma\eta},$$
$$f_0(0) = 0, \qquad f_1(0) = 1, \qquad \theta_0(0) = 1, \qquad f_1(\eta_\infty) = 0, \qquad \theta_0(\eta_\infty) = 0.$$

For validation, the current numerical results were compared with data of four references [3, 4, 24, 26] in some similar cases. All the results are in good agreement: the difference is not greater than 10^{-4} (Tables 1 and 2).

Table 1. Local skin friction coefficients $-f''(0)$ for different values of M and γ

M	$-f''(0)$					
	Data of Vajravelu et al. [26]			Present study		
	$\gamma = 0$	$\gamma = 0.5$	$\gamma = 1$	$\gamma = 0$	$\gamma = 0.5$	$\gamma = 1$
0	1.000001	1.182410	1.358198	1.000001	1.182410	1.358203
0.5	1.224745	—	—	1.224745	1.354751	1.499818
1.0	1.414214	—	—	1.414214	1.513473	1.634410
1.5	1.581139	—	—	1.581138	1.660637	1.762612
2.0	1.732051	—	—	1.732050	1.797992	1.884995

Table 2. Temperature gradients $-\theta'(0)$ for $\gamma = M = \mathrm{Ec} = N = 0$, $s = 1$, and different values of the Prandtl number

Pr	$-\theta'(0)$			
	Data of Grubka and Bobba [3]	Data of Ali [4]	Data of Ishak and Nazar [24]	Present study
0.10	—	—	—	0.2090
0.72	0.8086	0.8058	0.8086	0.8086
1.00	1.0000	0.9961	1.0000	1.0000
2.00	—	—	—	1.5231
3.00	1.9237	1.9144	1.9237	1.9236
5.00	—	—	—	2.5575
10.00	3.7207	3.7006	3.7207	3.7206

Table 3. Local skin friction coefficients $-f''(0)$ for different values of the transverse curvature and magnetic field parameters

M	$-f''(0)$				
	$\gamma = 0$	$\gamma = 0.25$	$\gamma = 0.50$	$\gamma = 0.75$	$\gamma = 1.00$
0	1.000001	1.091825	1.182410	1.271146	1.358203
0.5	1.224745	1.286865	1.354751	1.426281	1.499818
1.0	1.414214	1.460675	1.513473	1.571918	1.634410
1.5	1.581138	1.690141	1.660637	1.709124	1.762612
2.0	1.732050	1.818930	1.797992	1.838857	1.884995

RESULTS AND DISCUSSION

The problem of the flow and heat transfer of a Newtonian fluid over a stretching slender cylinder is analyzed numerically. The results of the solution are illustrated in Figs. 2–8 and Tables 3–5.

Figure 2 show the axial $f'(\eta)$ and transverse $f(\eta)$ velocity profiles for different values of the magnetic field parameter M and transverse curvature parameter γ. It is observed that an increase in the magnetic field parameter decreases the boundary layer thickness. This behavior can be due to the fact that the magnetic field induces the Lorentz force affecting the flow field. In addition, it can be seen from Fig. 2b that $f(\eta) \neq 0$ on the boundary layer edge. The skin friction coefficients $-f''(0)$ are listed in Table 3 for several values of the magnetic field parameter and surface curvature. As it follows from Table 3, an increase in the magnetic field parameter causes an increase in the skin friction coefficient, which is depicted in Fig. 3 for a range of Reynolds numbers and two different values of the transverse curvature parameter. For instance, an increase in the magnetic field parameter from 0 to 2 leads to an increase in the value of $-f''(0)$ by 38.78% in the case with $\gamma = 1$ and approximately by 73.2% in the case with $\gamma = 0$. Moreover, at $M = 0$–2, there is a regressive rate of the increase in the skin friction coefficient $-f''(0)$. This behavior is due to the fact that an increase in the magnetic field parameter decreases the axial velocity, which, in turn, decreases the value of the Lorentz force; as a result, the influence of the magnetic field parameter is diminished.

As it follows from Fig. 2, the boundary layer thickness in the case with $\gamma = 1$ is greater than that in the case with $\gamma = 0$, which means that the velocity increases with an increase in the transverse curvature of the surface. An interesting point is that the transverse curvature parameter and the magnetic field parameter produce similar effects on the skin friction coefficient.

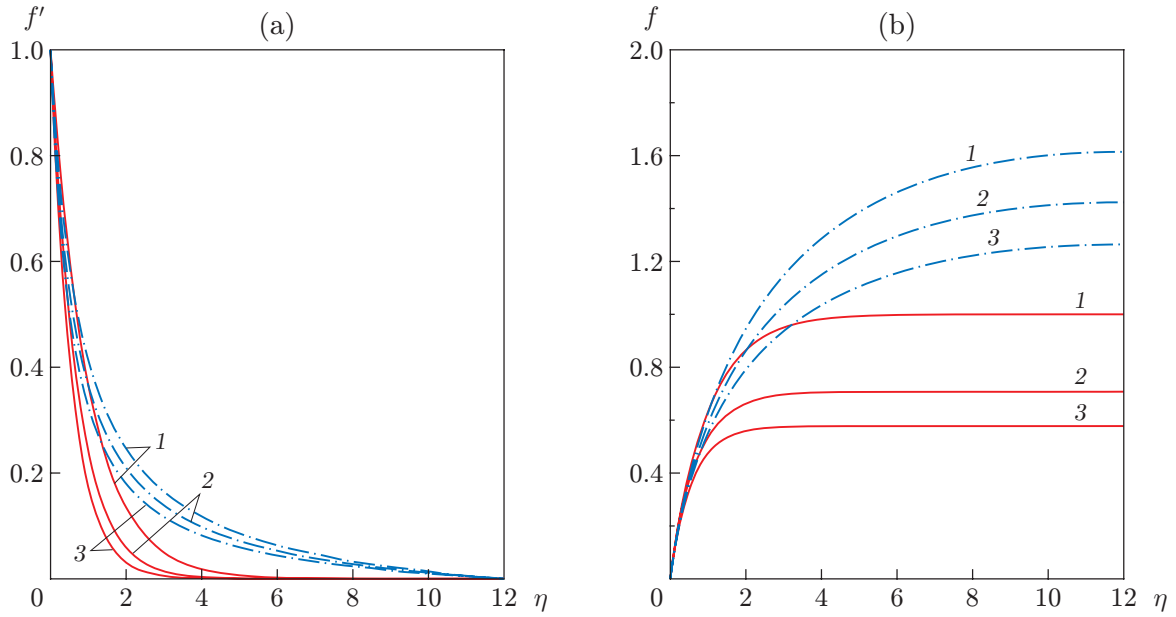

Fig. 2. Axial (a) and transverse (b) velocity profiles for different values of γ and M: the solid and dot-and-dashed curves show the results for $\gamma = 0$ and 1, respectively; $M = 0$ (*1*), 1 (*2*), and 2 (*3*).

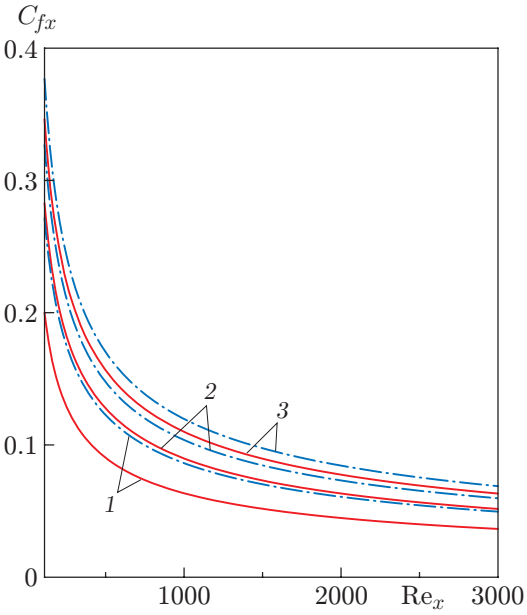

Fig. 3.

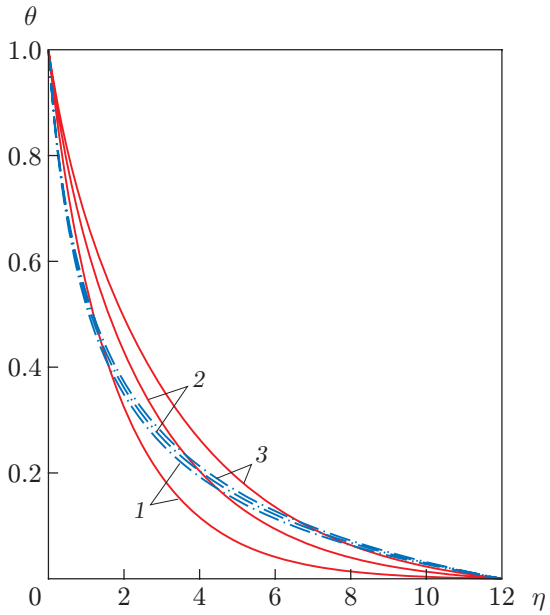

Fig. 4.

Fig. 3. Local skin friction coefficient versus the local Reynolds number for different values of γ and M (notation the same as in Fig. 2).

Fig. 4. Temperature profiles for $s = 1$, $\mathrm{Pr} = 1$, $N = 1$, $\mathrm{Ec} = 0.02$, and different values of γ and M (notation the same as in Fig. 2).

Table 4. Wall temperature gradients $-\theta'(0)$ for different values of parameters

M	Ec	N	s	Pr	$-\theta'(0)$	
					$\gamma = 0$	$\gamma = 1$
0	0.02	1.0	1.0	1.0	0.6273	1.0231
0.5	0.02	1.0	1.0	1.0	0.5723	1.0084
1.0	0.02	1.0	1.0	1.0	0.5302	0.9945
1.5	0.02	1.0	1.0	1.0	0.4968	0.9815
2.0	0.02	1.0	1.0	1.0	0.4691	0.9694
1.0	0	1.0	1.0	1.0	0.5364	1.0015
1.0	1.00	1.0	1.0	1.0	0.2244	0.6518
1.0	2.00	1.0	1.0	1.0	−0.0876	0.3020
1.0	3.00	1.0	1.0	1.0	−0.3997	−0.0478
1.0	4.00	1.0	1.0	1.0	−0.7119	−0.3976
1.0	0.02	0	1.0	1.0	0.8806	1.3035
1.0	0.02	0.5	1.0	1.0	0.6578	1.1036
1.0	0.02	1.0	1.0	1.0	0.5302	0.9945
1.0	0.02	1.5	1.0	1.0	0.4476	0.9258
1.0	0.02	2.0	1.0	1.0	0.3901	0.8784
1.0	0.02	2.5	1.0	1.0	0.3479	0.8438
1.0	0.02	3.0	1.0	1.0	0.3157	0.8175
1.0	0.02	1.0	1.0	1.0	0.5302	0.9945
1.0	0.02	1.0	2.0	1.0	0.7424	1.2025
1.0	0.02	1.0	3.0	1.0	0.9311	1.3878
1.0	0.02	1.0	4.0	1.0	1.1016	1.5558
1.0	0.02	1.0	5.0	1.0	1.2577	1.7098
1.0	0.02	1.0	1.0	0.1	0.1299	0.6622
1.0	1.00	1.0	1.0	1.0	0.5302	0.9945
1.0	1.00	1.0	1.0	2.0	0.8806	1.3035
1.0	1.00	1.0	1.0	3.0	1.1584	1.5670
1.0	1.00	1.0	1.0	5.0	1.6002	2.0029
1.0	1.00	1.0	1.0	10.0	2.4082	2.8115

The effect of the magnetic field parameter on the temperature field is illustrated in Fig. 4. With an increase in the magnetic field parameter, the wall temperature gradient decreases; consequently, the major part of heat is transmitted to the fluid near the boundary layer edge, resulting in an increase in temperature. According to the numerical results presented in Table 4, an increase in the magnetic field parameter from 0 to 2 induces a decrease in $-\theta'(0)$ by 5.25 and 25.22% for the cases with $\gamma = 1$ and $\gamma = 0$, respectively.

Figure 5 illustrates the influence of viscous dissipation on the temperature field for different values of the Eckert number. It is seen that the temperature profile grows with an increase in the Eckert number. Also, it is observable from Table 4 that the wall temperature gradient decreases with increasing Eckert number, whereas the temperature increases. Another valuable remark is that the temperature gradient changes its sign if the Eckert number is increased above a particular critical value. In this case, the viscous dissipation mechanism acts as a heat source and produces thermal energy in the flow, which is responsible for this change in the sign of the wall temperature gradient. This critical value of the Eckert number depends on the magnetic field parameter M, Prandtl number Pr, thermal radiation parameter N, and surface temperature exponent s (Table 5). The critical Eckert number is seen to decrease with increasing magnetic field parameter and Prandtl number. On the other hand, the critical Eckert number increases with an increase in the thermal radiation parameter, which is also true about the role of the surface temperature exponent.

Figure 6 demonstrates the effect of thermal radiation on the fluid temperature profile: the temperature increases with an increase in the radiation parameter value. According to Table 4, as the radiation parameter increases from 0 to 2, the wall temperature gradient decreases by 55.7% in the case with $\gamma = 0$ and by 32.61% in the case with $\gamma = 1$.

Figure 7 displays the role of the surface temperature exponent s on the temperature profile. It is clear that an increase in the surface temperature exponent leads to a greater wall temperature gradient. According to Table 4, the wall temperature gradient increases by 75.63 and 39.55% in the cases with $\gamma = 0$ and 1, respectively, as the surface temperature exponent s increases from 1 to 3.

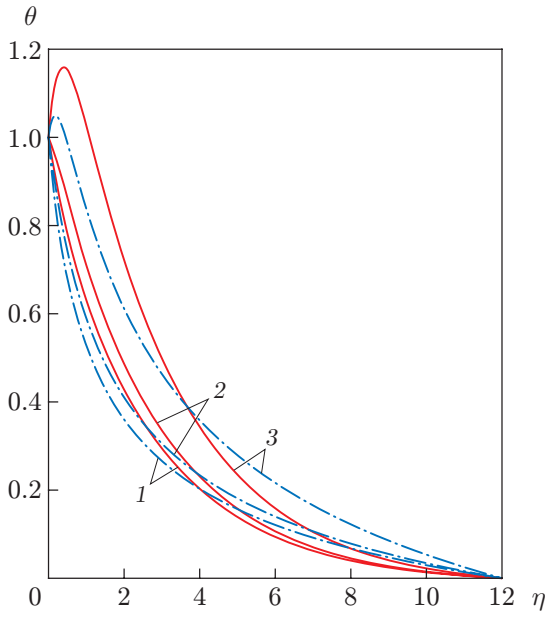

Fig. 5.

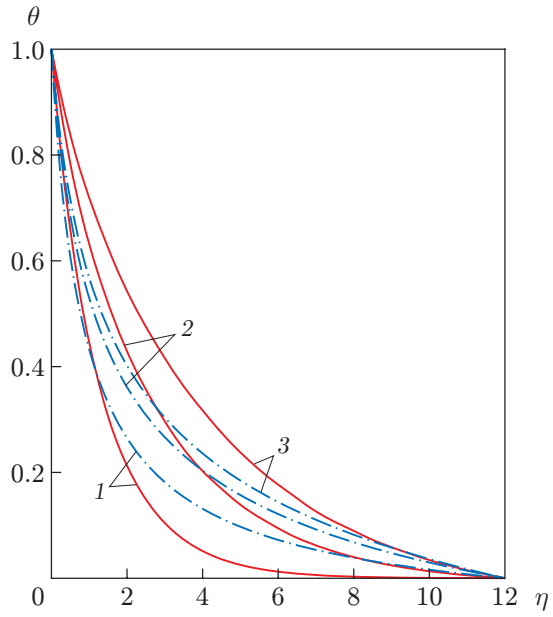

Fig. 6.

Fig. 5. Temperature profiles for $M = 1$, $s = 1$, $\mathrm{Pr} = 1$, $N = 1$, and different values of γ and Ec: the solid and dot-and-dashed curves show the results for $\gamma = 0$ and 1, respectively; $\mathrm{Ec} = 0$ (*1*), 1 (*2*), and 5 (*3*).

Fig. 6. Temperature profiles for $M = 1$, $s = 1$, $\mathrm{Pr} = 1$, $\mathrm{Ec} = 0.02$, and different values of γ and N: the solid and dot-and-dashed curves show the results for $\gamma = 0$ and 1, respectively; $N = 0$ (*1*), 1 (*2*), and 2 (*3*).

Table 5. Eckert numbers for $\theta'(0) = 0$ and different values of parameters

M	Pr	N	s	Ec	
				$\gamma = 0$	$\gamma = 1$
1.0	1.0	1.0	1.0	1.7190	2.8634
2.0	1.0	1.0	1.0	1.2076	2.4319
1.0	2.0	1.0	1.0	1.5438	1.9936
1.0	1.0	2.0	1.0	1.8379	3.7070
1.0	1.0	1.0	2.0	2.5187	3.6159

The effect of the Prandtl number on the temperature profile is plotted in Fig. 8. Obviously, the result of using fluids with higher Prandtl numbers is the lower temperature. The data in Table 4 confirm the commonly known claim that fluids with higher Prandtl numbers have greater wall temperature gradients and, as a consequence, lower temperatures.

The effect of the transverse curvature parameter γ on the temperature profiles is illustrated in Figs. 4–8 and Table 4. In all cases, an increase in the surface transverse curvature leads to an increase not only in the wall temperature gradient, but also in the temperature profiles. This phenomenon may be due to the fact that an increase in the surface transverse curvature leads to an increase in the boundary layer thickness and, as a consequence, in the temperature and velocity profiles.

CONCLUSIONS

The flow and heat transfer of a fluid over a stretching slender cylinder in the presence of an external radial magnetic field and different transverse curvatures is studied numerically; the effects of viscous dissipation, thermal radiation, Prandtl number, and different prescribed surface temperature exponents on the temperature profile are examined. The following remarks can be made as a result of this study.

An increase in the magnetic field parameter from 0 to 2 leads to a decrease in the velocity profile, whereas the skin friction coefficient increases by 38.78% in the case with $\gamma = 1$ and approximately by 73.2% in the case with

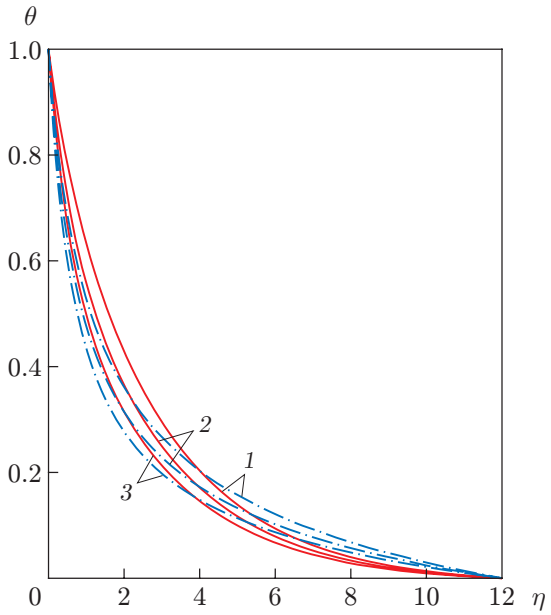

Fig. 7.

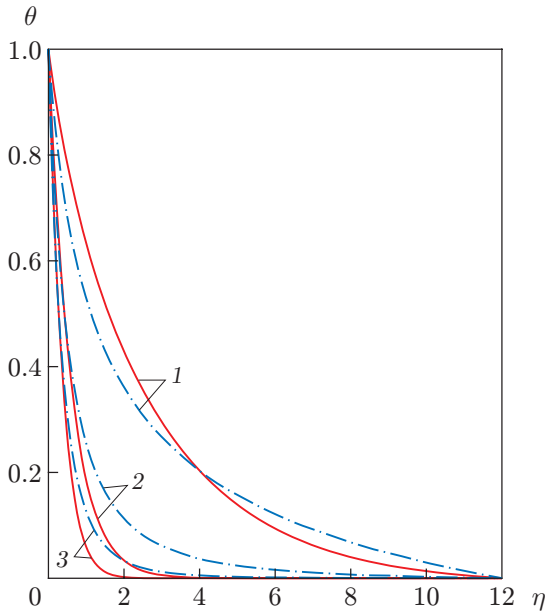

Fig. 8.

Fig. 7. Temperature profiles for $M = 1$, $\mathrm{Pr} = 1$, $N = 1$, $\mathrm{Ec} = 0.02$, and different values of γ and s: the solid and dot-and-dashed curves show the results for $\gamma = 0$ and 1, respectively; $s = 1$ (*1*), 2 (*2*), and 3 (*3*).

Fig. 8. Temperature profiles for $M = 1$, $s = 1$, $N = 1$, $\mathrm{Ec} = 0.02$, and different values of γ and Pr: the solid and dot-and-dashed curves show the results for $\gamma = 0$ and 1, respectively; $\mathrm{Pr} = 1$ (*1*), 5 (*2*), and 10 (*3*).

$\gamma = 0$.

An increase in the magnetic field parameter from 0 to 2 causes a rise in the temperature profile, while the wall temperature gradient decreases by 5.25 and 25.22% in the cases with $\gamma = 1$ and $\gamma = 0$, respectively.

The wall temperature gradient decreases with an increase in the Eckert number, whereas the temperature increases. In addition, there is a particular critical value of the Eckert number at which the wall temperature gradient is equal to zero.

An increase in the thermal radiation parameter from 0 to 3 leads to enhancement of the temperature profile and to a decrease in the wall temperature gradient.

An increase in the surface temperature exponent from 1 to 5 reduces the temperature profile and increases the wall temperature gradient.

REFERENCES

1. L. J. Crane, "Flow Past a Stretching Plate," Z. Angew. Math. Phys. **21**, 645–647 (1970).
2. P. S. Gupta and A. S. Gupta, "Heat and Mass Transfer on a Stretching Sheet with Suction or Blowing," Canad. J. Chem. Eng. **55**, 744–746 (1977).
3. L. J. Grubka and K. M. Bobba, "Heat Transfer Characteristics of a Continuous, Stretching Surface with Variable Temperature," J. Heat Transfer **107**, 248–250 (1985).
4. M. E. Ali, "Heat Transfer Characteristics of a Continuous Stretching Surface," Heat Mass Transfer **29**, 227–234 (1994).
5. C. Y. Wang, "Liquid Film on an Unsteady Stretching Surface," Quart. Appl. Math. **48**, 601–610 (1990).
6. H. I. Andersson and B. S. Dandapat, "Flows of a Power Law Fluid over a Stretching Sheet," Stability Appl. Anal. Continuous Media **1**, 339–347 (1991).
7. H. I. Andersson, J. B. Aarseth, N. Braud, and B. S. Dandapat, "Flow of a Power-Law Fluid Film on an Unsteady Stretching Surface," J. Non-Newton. Fluid Mech. **62**, 1–8 (1996).
8. C. H. Chen, "Heat Transfer in a Power-Law Fluid Film over a Unsteady Stretching Sheet," Heat Mass Transfer **39**, 791–796 (2003).

9. A. J. Chamkha, "Unsteady Hydromagnetic Flow and Heat Transfer from a Non-Isothermal Stretching Sheet Immersed in a Porous Medium," Int. Comm. Heat Mass Transfer. **25**, 899–906 (1998).
10. M. S. Abel, N. Mahesha, and J. Tawade, "Heat Transfer in a Liquid Film over an Unsteady Stretching Surface with Viscous Dissipation in Presence of External Magnetic Field," Appl. Math. Model. **33**, 3430–3441 (2009).
11. S. Mukhopadhyay, "Effect of Thermal Radiation on Unsteady Nixed Convection Flow and Heat Transfer over a Porous Stretching Surface in Porous Medium," Int. J. Heat Mass Transfer **52**, 3261–3265 (2009).
12. S. Mukhopadhyay, "Unsteady Boundary Layer Flow and Heat Transfer Past a Porous Stretching Sheet in Presence of Variable Viscosity and Thermal Diffusivity," Int. J. Heat Mass Transfer **52**, 5213–5217 (2009).
13. R. Tsai, K. H. Huang, and J. S. Huang, "Flow and Heat Transfer over an Unsteady Stretching Surface with non-Uniform Heat Source," Int. Comm. Heat Mass Transfer **35**, 1340–1343 (2008).
14. C.-H. Chen, "Effect of Viscous Dissipation on Heat Transfer in a non-Newtonian Liquid Film over an Unsteady Stretching Sheet," J. Non-Newton. Fluid Mech. **135**, 128–135 (2006).
15. C.-H. Chen, "Effects of Magnetic Field and Suction/Injection on Convection Heat Transfer of non-Newtonian Power-Law Fluids Past a Power-Law Stretched Sheet with Surface Heat Flux," Int. J. Thermal. Sci. **47**, 954–961 (2008).
16. R. Cortell, "Effects of Viscous Dissipation and Radiation on the Thermal Boundary Layer over a Nonlinearly Stretching Sheet," Phys. Lett. A **372**, 631–636 (2008).
17. K. H. Huang, R. Tsai, and C. H. Huang, "Chebyshev Finite Difference Approach to Modeling the Thermoviscosity Effect in a Power-Law Liquid Film on an Unsteady Stretching Surface," Non-Newton. Fluid Mech. **165**, 1351–1356 (2010).
18. K. Vajravelu, K. V. Prasad, and C.-O. Ng, "Unsteady Flow and Heat Transfer in a Thin Film of Ostwald–de Waele Liquid over a Stretching Surface," Comm. Nonlinear Sci. Numer. Simulat. **17**, 4163–4173 (2012).
19. L. J. Crane, "Boundary Layer Flow due to a Stretching Cylinder," Z. Angew. Math. Phys. **26**, 619–622 (1975).
20. C. Y. Wang, "Fluid Flow due to a Stretching Cylinder," Phys. Fluids **31**, 466–468 (1988).
21. A. Ishak, R. Nazar, and I. Pop, "Uniform Suction/Blowing Effect on Flow and Heat Transfer due to a Stretching Cylinder," Appl. Math. Model. **32**, 2059–2066 (2008).
22. A. Ishak, R. Nazar, and I. Pop, "Magnetohydrodynamic (MHD) Flow and Heat Transfer due to a Stretching Cylinder," Energy Convers Manag. **49**, 3265–3269 (2008).
23. W. M. K. A. Wan Zaimi, A. Ishak, and I. Pop, "Unsteady Viscous Flow over a Shrinking Cylinder," J. King Saud Univ. Science **25**, 143–148 (2013).
24. A. Ishak and R. Nazar, "Laminar Boundary Layer Flow along a Stretching Cylinder," Europ. J. Sci. Res. **36**, 22–29 (2009).
25. N. Bachok and A. Ishak, "Flow and Heat Transfer over a Stretching Cylinder with Prescribed Surface Heat Flux," Malays. J. Math. Sci. **4**, 159–169 (2010).
26. K. Vajravelu, K. V. Prasad, and S. R. Santhi, "Axisymmetric Magneto-Hydrodynamic (MHD) Flow and Heat Transfer at a Non-isothermal Stretching Cylinder," Appl. Math. Comput. **219**, 3993–4005 (2012).
27. S. Mukhopadhyay, "Mixed Convection Boundary Layer Flow along a Stretching Cylinder in Porous Medium," J. Petroleum Sci. Eng. **96/97**, 73–78 (2012).
28. P. M. Patil, S. Roy, and I. Pop, "Unsteady Effects on Mixed Convection Boundary Layer Flow from a Permeable Slender Cylinder due to non-Linearly Power Law Stretching," Comput. Fluids **56**, 17–23 (2012).
29. J. A. Shercliff, *A Textbook of Magnetohydrodynamics* (Pergamon Press, 1965).
30. M. Q. Brewster, *Thermal Radiative Transfer and Properties* (John Wiley, New York, 1992).